

CRACK PROBLEMS FOR BONDED NONHOMOGENEOUS
MATERIALS UNDER ANTIPLANE SHEAR LOADING

by

F. Erdogan

September 1984

Lehigh University, Bethlehem, PA

The National Aeronautics and Space Administration

Grant No. NGR 39 007 011

THE CRACK PROBLEM FOR BONDED NONHOMOGENEOUS
MATERIALS UNDER ANTIPLANE SHEAR LOADING

F. Erdogan
Lehigh University, Bethlehem, PA 18015

ABSTRACT

The main objective of this paper is the investigation of the singular nature of the crack tip stress field in a nonhomogeneous medium having a shear modulus with a discontinuous derivative. The problem is considered for the simplest possible loading and geometry, namely the antiplane shear loading of two bonded half spaces in which the crack is perpendicular to the interface. It is shown that the square-root singularity of the crack tip stress field is unaffected by the discontinuity in the derivative of the shear modulus. The problem is solved for a finite crack and extensive results are given for the stress intensity factors.

1. Introduction

In a nonhomogeneous medium if the elastic moduli are piecewise constant, it is known that the stress field around a crack tip terminating at the interface has a behavior of the form r^α where r is the distance from the crack tip and $-1 < \alpha < 0$ (see, for example, [1] and [2]). It is also known that if the nonhomogeneous medium has elastic moduli which are continuous with continuous derivatives the stress state around the crack tips has the standard square-root singularity [3], [4]. What has not been studied so far is the effect of the discontinuity of the derivatives of elastic moduli on the crack tip stress singularity for a crack terminating at the plane of discontinuity. In this paper the problem is studied for the simple case of antiplane shear loading of an infinite medium in which the shear modulus μ is a function of x only, $d\mu/dx$ is discontinuous along the $x=0$ plane, and the crack lies in the xz plane (Fig. 1). The main objective of the paper is to investigate the effect of $d\mu/dx$ on the stress singularity. Hence, it is further assumed that μ is an exponential function in x , which appears to lead to a relatively simple formulation of the problem.

2. Formulation of the Problem

The antiplane shear problem for the nonhomogeneous medium shown in Fig. 1 having the elastic properties

$$\mu(x) = \mu_0 e^{\beta x}, \quad x > 0; \quad \mu(x) = \mu_0 e^{\gamma x}, \quad x < 0, \quad (1)$$

may be formulated as follows:

$$\nabla^2 w_1 + \beta \frac{\partial w_1}{\partial x} = 0, \quad 0 < x < \infty, \quad 0 \leq y < \infty, \quad (2)$$

$$\nabla^2 w_2 + \gamma \frac{\partial w_2}{\partial x} = 0, \quad -\infty < x < 0, \quad 0 \leq y < \infty \quad (3)$$

$$w_1(0, y) = w_2(0, y), \quad (4)$$

$$\sigma_{1xz}(0, y) = \sigma_{2xz}(0, y), \quad (5)$$

$$w_1(x, 0) = 0, \quad 0 \leq x < a, \quad b < x < \infty, \quad (6)$$

$$\sigma_{1yz}(x, +0) = p(x), \quad a < x < b, \quad (7)$$

where it is assumed that the crack surface traction $p(x)$ is the only nonzero external load and that because of symmetry it is sufficient to consider the problem for $y > 0$ only. Expressing the solution of (2) and (3) as

$$w_1(x, y) = \frac{1}{2\pi} \int_{-\infty}^{\infty} f_1(y, \alpha) e^{-i\alpha x} d\alpha + \frac{2}{\pi} \int_0^{\infty} g_1(x, \alpha) \sin y \alpha d\alpha, \quad (8)$$

$$w_2(x, y) = \frac{2}{\pi} \int_0^{\infty} g_2(x, \alpha) \sin y \alpha d\alpha, \quad (9)$$

we obtain

$$f_1 = A(\alpha) e^{m y}, \quad g_1 = B(\alpha) e^{n x}, \quad g_2 = C(\alpha) e^{\lambda x},$$

$$m = -\sqrt{\alpha^2 + i\beta\alpha}, \quad n = -\alpha_1 - \frac{\beta}{2}, \quad \lambda = \alpha_2 - \frac{\gamma}{2},$$

$$\alpha_1 = \sqrt{\alpha^2 + \beta^2/4}, \quad \alpha_2 = \sqrt{\alpha^2 + \gamma^2/4}. \quad (10)$$

The stress components are given by

$$\sigma_{1xz} = \mu_0 e^{\beta x} \frac{\partial w_1}{\partial x}, \quad \sigma_{1yz} = \mu_0 e^{\beta x} \frac{\partial w_1}{\partial y}, \quad (0 < x < \infty, 0 < y < \infty), \quad (11)$$

$$\sigma_{2xz} = \mu_0 e^{\gamma x} \frac{\partial w_2}{\partial x}, \quad \sigma_{2yz} = \mu_0 e^{\gamma x} \frac{\partial w_2}{\partial y}, \quad (-\infty < x < 0, 0 < y < \infty). \quad (12)$$

Substituting from (8)-(12) into the continuity conditions (4) and (5) it may easily be shown that

$$C(\alpha) - B(\alpha) = \frac{1}{2\pi} \int_{-\infty}^{\infty} \frac{\alpha A(\rho) d\rho}{\alpha^2 + \rho^2 + i\beta\rho}, \quad (13)$$

$$nB(\alpha) - \lambda C(\alpha) = \frac{1}{2\pi} \int_{-\infty}^{\infty} \frac{i\alpha\rho A(\rho) d\rho}{\alpha^2 + \rho^2 + i\beta\rho}. \quad (14)$$

Defining now

$$g(x) = \frac{\partial}{\partial x} w_1(x, 0), \quad (15)$$

from (8), (10) and (6) we find

$$i\alpha A(\alpha) = - \int_a^b g(t) e^{i\alpha t} dt, \quad (16)$$

$$\int_a^b g(t) dt = 0. \quad (17)$$

By substituting from (16) into (13) and (14) and by using the residue theorem to evaluate the improper integrals and the condition (17), the unknown functions B and C may be obtained as follows:

$$B(\alpha) = \frac{\alpha(\alpha_1 - \alpha_2 + \frac{\gamma - \beta}{2})}{2\alpha_1(\lambda - n)(\alpha_1 - \beta/2)} \int_a^b g(t) e^{-t(\alpha_1 - \beta/2)} dt, \quad (18)$$

$$C(\alpha) = \frac{\alpha}{(\lambda-n)(\alpha_1-\beta/2)} \int_a^b g(t) e^{-t(\alpha_1-\beta/2)} dt \quad (19)$$

Thus, $g(t)$ is the only unknown in the problem which may be determined from the remaining boundary condition (7). From (7), (8), (10), (11), (16) and (18) it then follows that

$$\sigma_{1yz}(x,0) = p(x) = \mu_0 e^{\beta x} \frac{1}{\pi} \int_a^b [k_1(x,t) + k_2(x,t)] g(t) dt, \quad a < x < b, \quad (20)$$

$$k_1(x,t) = \lim_{y \rightarrow +0} \frac{i}{2} \int_{-\infty}^{\infty} \frac{m(\alpha)}{\alpha} e^{m\alpha y} e^{i\alpha(t-x)} d\alpha, \quad (21)$$

$$k_2(x,t) = \lim_{y \rightarrow +0} e^{(t-x)\beta/2} \int_0^{\infty} \frac{\alpha^2(\alpha_1-\alpha_2 + \frac{y-\beta}{2})}{\alpha_1(\lambda-n)(\alpha_1 - \frac{\beta}{2})} e^{-(t+x)\alpha_1} \cos \alpha y dx. \quad (22)$$

Referring to (10) and the regularity conditions at infinity it may be noted that $\text{Re}(m) < 0$, $\text{Re}(n) < 0$ and $\text{Re}(\lambda) > 0$. The singular behavior of the kernels k_1 and k_2 may be obtained from the asymptotic analysis of the integrals in (21) and (22). By observing that for large values of α , $m(\alpha) \rightarrow -|\alpha|$, from (21) we find

$$k_1(x,t) = \lim_{y \rightarrow +0} \frac{i}{2} \int_{-\infty}^{\infty} \frac{-|\alpha|}{\alpha} e^{-|\alpha|y} e^{i\alpha(t-x)} d\alpha + \frac{i}{2} \int_{-\infty}^{\infty} \left(\frac{m}{\alpha} + \frac{|\alpha|}{\alpha} \right) e^{i\alpha(t-x)} d\alpha \quad (23)$$

where because of uniform convergence, in the second integral the limit has been put under the integral. By evaluating the first integral k_1 is obtained as follows:

$$k_1(x,t) = \frac{1}{t-x} + h_1(x,t), \quad (24)$$

$$h_1(x,t) = \text{Im} \left\{ \int_0^{\infty} \left(\sqrt{1 + \frac{i\beta}{\alpha}} - 1 \right) e^{i\alpha(t-x)} d\alpha \right\} . \quad (25)$$

where the function h_1 is bounded for all values of x and t in the closed interval $[a,b]$, $a \geq 0$.

Similar asymptotic analysis would show that the kernel k_2 is bounded for $a > 0$ (for which $t+x > 0$), and has only a logarithmic end point singularity for $a=0$ (i.e., for $x+t \rightarrow 0$). We first write

$$k_2(x,t) = e^{(t-x)\beta/2} \int_0^{\infty} K_2(x,t,\alpha) \cos \alpha y d\alpha , \quad (26)$$

$$K_2(x,t,\alpha) = \frac{\alpha^2(\alpha_1 - \alpha_2 + \frac{\gamma - \beta}{2})}{\alpha_1(\lambda - n)(\alpha_1 - \beta/2)} e^{-(t+x)\alpha_1} . \quad (27)$$

The limiting behavior of the integrand K_2 for $\alpha \rightarrow 0$ and for $\alpha \rightarrow \infty$ is

$$K_2 \rightarrow K_{20}(x,t,\alpha) = \frac{2(\gamma - \beta)}{\gamma\beta^2} \alpha^2 e^{-(t+x)\beta/2} , \text{ for } \alpha \rightarrow 0 , \quad (28)$$

$$K_2 \rightarrow K_{2\infty}(x,t,\alpha) = \frac{\gamma - \beta}{4} \frac{1}{\alpha} e^{-\alpha(t+x)} , \text{ for } \alpha \rightarrow \infty . \quad (29)$$

We now express k_2 as

$$k_2(x,t) = \lim_{y \rightarrow +0} e^{(t-x)\beta/2} \left[\int_0^{\epsilon} K_{20}(x,t,\alpha) \cos \alpha y d\alpha + \int_{\epsilon}^N K_2(x,t,\alpha) \cos \alpha y d\alpha + \int_N^{\infty} K_{2\infty}(x,t,\alpha) \cos \alpha y d\alpha + \delta \right] \quad (30)$$

where ϵ is a very small and N is a very large constant and the constant δ may be made as small as we please by selecting ϵ sufficiently small and N sufficiently large. Note that in $\epsilon \leq \alpha \leq N$ K_2 is bounded and hence, the second integral in (30) is finite for all $x \geq 0$, $t \geq 0$. Equation (28) shows that the same is true also for the first integral in (30). The third integral is the exponential integral which may be expanded as

$$\lim_{y \rightarrow +0} \int_N^{\infty} \frac{e^{-\alpha(t+x)}}{\alpha} \cos \alpha y d\alpha = \lim_{y \rightarrow 0^+} \operatorname{Re}\{Ei[(t+x-iy)N]\} = -\log(t+x) - \log N - \gamma_0$$

$$- \frac{N^2}{2 \cdot 2!} (t+x)^2 + \frac{N^3}{3 \cdot 3!} (t+x)^3 - \dots \quad (31)$$

where γ_0 is the Euler's constant. One may note that if N is nonzero and finite then the exponential integral in (31) and consequently the kernel k_2 is bounded for all x and t in $0 < (x,t) < b$ and has only a logarithmic singularity at $x=0=t$. Since the kernel $\log(t+x)$ is square integrable, it may thus be concluded that the dominant part of the integral equation (20) has only a simple Cauchy kernel for $a=0$ as well as $a>0$, and the solution is of the form [5]

$$g(t) = \frac{G(t)}{\sqrt{(t-a)(b-t)}} \quad , \quad (0 \leq a < t < b) \quad . \quad (32)$$

3. Stress Intensity Factors

For $a>0$ we observe that (20) gives $\sigma_{1yz}(x,0)$ for $0 < x < \infty$ and the function F defined by

$$F(x) = \int_a^b [h_1(x,t) + k_2(x,t)]g(t)dt \quad (33)$$

is bounded in the closed interval $a \leq x \leq b$. Thus (20) may be expressed as

$$\frac{1}{\mu_0} e^{-\beta x} \sigma_{1yz}(x,0) = \frac{i}{\pi} \int_a^b \frac{G(t)dt}{(t-x)X^+(t)} + F(x) \quad , \quad (0 < x < \infty) \quad (34)$$

where

$$X(z) = \sqrt{(z-a)(z-b)} \quad , \quad X^+(t) = -X^-(t) = \sqrt{(t-a)(t-b)} \quad , \quad (z=x+iy) \quad . \quad (35)$$

Consider now the function

$$\phi(z) = \frac{1}{2\pi i} \oint_C \frac{G(s)ds}{(s-z)X(s)} \quad (36)$$

where the contour C encircles the crack and z is outside C. By shrinking the contour to the cut, from (34)-(36) it may be shown that

$$\frac{1}{\mu_0} e^{-\beta x} \sigma_{1yz}(x,0) = -\phi(x) + F(x), \quad (0 < x < a, b < x < \infty) . \quad (37)$$

On the other hand, from (36) it follows that [5]

$$\phi(z) = \frac{G(z)}{X(z)} - P(z) \quad (38)$$

where P(z) is the principal part of G/X at $|z| = \infty$. From (37) and (38) we find

$$\frac{1}{\mu_0} e^{-\beta x} \sigma_{1yz}(x,0) = -\frac{G(x)}{X(x)} + P(x) + F(x), \quad (0 < x < a, b < x < \infty) . \quad (39)$$

By observing that

$$X(x) = \sqrt{(x-b)(x-a)}, \quad (x > b); \quad X(x) = -\sqrt{(a-x)(b-x)}, \quad (x < a) , \quad (40)$$

the Mode III stress intensity factors at the crack tips may now be defined and expressed as follows:

$$\begin{aligned} k_3(b) &= \lim_{x \rightarrow b} \sqrt{2(x-b)} \sigma_{1yz}(x,0) = -\mu_0 e^{\beta b} \frac{G(b)}{\sqrt{(b-a)/2}} \\ &= -\lim_{x \rightarrow b} \mu(x) \sqrt{2(b-x)} g(x) , \end{aligned} \quad (41)$$

$$\begin{aligned} k_3(a) &= \lim_{x \rightarrow a} \sqrt{2(a-x)} \sigma_{1yz}(x,0) = \mu_0 e^{\beta a} \frac{G(a)}{\sqrt{(b-a)/2}} \\ &= \lim_{x \rightarrow a} \mu(x) \sqrt{2(x-a)} g(x) . \end{aligned} \quad (42)$$

For $a=0$ we define the stress intensity factor at the crack tip $x=0$ as follows:

$$k_3(0) = \lim_{x \rightarrow 0} \sqrt{-2x} \sigma_{2yz}(x,0) . \quad (43)$$

To calculate $k_3(0)$ the asymptotic analysis of σ_{2yz} around the crack tip $x=0$ is needed. From (9), (12) and (19) σ_{2yz} may be expressed as

$$\begin{aligned}\sigma_{2yz}(x,y) &= \mu_0 e^{\gamma x} \frac{2}{\pi} \int_0^{\infty} C(\alpha) e^{\lambda x} \alpha \cos \alpha y d\alpha \\ &= \mu_0 e^{\gamma x} \frac{1}{\pi} \int_0^b h_3(x,t) g(t) e^{(\beta t - \gamma x)/2} dt\end{aligned}\quad (44)$$

where

$$h_3(x,t) = \lim_{y \rightarrow +0} 2 \int_0^{\infty} \frac{\alpha^2 e^{\alpha_2 x - \alpha_1 t} \cos \alpha y}{(\lambda - n)(\alpha_1 - \beta/2)} d\alpha.\quad (45)$$

By observing that $\alpha_1 \rightarrow \alpha$, $\alpha_2 \rightarrow \alpha$, $\lambda \rightarrow \alpha$ and $n \rightarrow -\alpha$ for $\alpha \rightarrow \infty$, from (45) we obtain

$$\begin{aligned}h_3(x,t) &= \lim_{y \rightarrow +0} \int_0^{\infty} e^{-\alpha(t-x)} \cos \alpha y d\alpha \\ &+ \int_0^{\infty} \left[\frac{2\alpha^2 e^{\alpha_2 x - \alpha_1 t}}{(\lambda - n)(\alpha_1 - \beta/2)} - e^{-\alpha(t-x)} \right] d\alpha\end{aligned}\quad (46)$$

where the second integral is uniformly convergent. Note that in (46) $t > 0$, $x < 0$ and $t - x > 0$. Thus, from

$$\lim_{y \rightarrow +0} \int_0^{\infty} e^{-\alpha(t-x)} \cos \alpha y d\alpha = \lim_{y \rightarrow +0} \frac{t-x}{(t-x)^2 + y^2} = \frac{1}{t-x},\quad (47)$$

and (46), σ_{2yz} may be obtained as follows:

$$\sigma_{2yz}(x,0) = \mu_0 e^{\gamma x/2} \frac{1}{\pi} \int_0^b \left[\frac{1}{t-x} + H_3(x,t) \right] g(t) e^{\beta t/2} dt,\quad (48)$$

where the bounded kernel H_3 is given by the second integral in (46).

If we now substitute from (32) into (48) and follow an analysis similar to (33)-(40), the asymptotic expression for σ_{2yz} may be written as

$$\sigma_{2yz}(x,0) = \mu_0 e^{\gamma x/2} \frac{G(x) e^{\beta x/2}}{\sqrt{(-x)(b-x)}} + K(x)\quad (49)$$

where K is a bounded function. Thus, from (49) and the definition of the stress intensity factor at $x=0$ as given by (43) it follows that

$$k_3(0) = \mu_0 \frac{G(0)}{\sqrt{b/2}} = \lim_{x \rightarrow 0} \mu(x) \sqrt{2x} g(x) \quad (50)$$

The results obtained in this section clearly show that the square-root character of the crack tip singularity is unaffected by the discontinuity in the derivative of the shear modulus.

From (10) and (22) it may be seen that for $\gamma=\beta$ (i.e., for the case of single nonhomogeneous plane) the kernel k_2 is identically zero and the expressions (24) and (25) defining k_1 remain unchanged. Thus, with $k_2=0$, (20), (24) and (25) give the density function $g(x)$ as defined by (32) and the stress intensity factors are then obtained from (41) and (42).

4. The Rigid Half Space

In the special case of an elastic half space bonded to a rigid half space, $w_2=0$, (8) is still valid and A and B are given by (16) and (13) (with $C=0$), respectively. Following an analysis similar to that of Section 2 (equations (20)-(31)), it may easily be shown that in this case the integral equation (20) becomes

$$p(x) = \mu_0 e^{\beta x} \frac{1}{\pi} \int_a^b \left[\frac{1}{t-x} + h_1(x) - \frac{1}{t+x} e^{\beta(t-x)/2} - h_2(x,t) e^{\beta(t-x)/2} \right] g(t) dt, \quad (a < x < b) \quad (51)$$

where h_1 is given by (25) and

$$h_2(x,t) = \int_0^{\infty} \left[\frac{\alpha^2}{\alpha_1(\alpha_1 - \frac{\beta}{2})} e^{-\alpha_1(t+x)} - e^{-\alpha(t+x)} \right] d\alpha \quad (52)$$

We note that for $\beta=0$ h_1 and h_2 vanish and (51) would reduce to the following known integral equation for the homogeneous half plane $x>0$ for which $w(0,y)=0$:

$$\frac{1}{\mu_0} p(x) = \frac{1}{\pi} \int_a^b \left(\frac{1}{t-x} - \frac{1}{t+x} \right) g(t) dt, \quad (a < x < b) \quad (53)$$

For $a > 0$, clearly the solution of (51) is of the form (32) and the solution may easily be obtained by following the technique described in, for example, [6]. In the limiting case of $a = 0$, by expressing the solution of (51) as

$$e^{\beta t} g(t) = G(t)(b-t)^{\omega_1} t^{\omega_2}, \quad (-1 < \text{Re}(\omega_1, \omega_2) \leq 0) \quad (54)$$

and by following the function theoretic method, it may easily be shown that (see, for example, [5] or [6])

$$G(b) \cot \pi \omega_1 = 0, \quad (55)$$

$$G(0) \left(\cot \pi \omega_2 - \frac{1}{\sin \pi \omega_2} \right) = 0. \quad (56)$$

Equations (55) and (56) are identical to the characteristic equations which would result from (53) and give $\omega_1 = -1/2$ and $\omega_2 = 0$ as the acceptable roots. It is, therefore, seen that at $t=0$ $g(t)$ is bounded. Physically, this result is indeed expected, as the half plane problem with $w_1(0, y) = 0$ corresponds to the antisymmetric problem for the infinite plane for which $\mu(x) = \mu_0 e^{\beta|x|}$ and which has a crack on the x axis along $-b < x < b$ subjected to antisymmetric shear tractions $\sigma_{yz}(x, 0) = p(x) = -p(-x)$, $(-b < x < b)$.

5. Results and Discussion

The calculated results are shown in Figures 2-4 and Tables 1 and 2. Figure 2 shows the stress intensity factors for an infinite plane with a shear modulus $\mu(x) = \mu_0 e^{\beta x}$ subjected to uniform shear tractions $\sigma_{1yz}(x, 0) = -p_0$. These results are analogous to those given in [4] for the pressurized crack. As in [4], the normalized stress intensity factors are independent of the crack location d (see Fig. 1) and are functions of the dimensionless parameter βc only. At first sight the result given in Fig. 2 to the effect that the stress intensity factor $k_3(a)$ on the stiffer side of the medium is greater than $k_3(b)$ may appear to be somewhat paradoxical. However, this result may easily be explained by considering the corresponding crack surface displacements given in Fig. 3 and obtained from

$$w_1(x, +0) = \int_0^x g(t) dt, \quad (0 < x < b). \quad (57)$$

The figure shows the normalized crack surface displacement $w_1(x,+0)$ for the nonhomogeneous infinite medium with $\mu(x) = \mu_0 \exp(\beta x)$, $\beta c = -2$, and for the homogeneous planes with shear moduli $\mu = \mu(0) = \mu_0$, $\mu = \mu(c) = \mu_0 \exp(-2)$ and $\mu = \mu(b) = \mu_0 \exp(-4)$. In the homogeneous planes the stress intensity factors are independent of μ and are given by

$$k_3(0) = k_3(b) = p_0 \sqrt{c} \quad , \quad (58)$$

whereas the crack surface displacement is inversely proportional to μ , i.e.

$$w(x,+0) = \frac{p_0}{\mu} \sqrt{x(b-x)} \quad , \quad (0 < x < b) \quad . \quad (59)$$

From Fig. 3 it is seen that near the crack tip $x=0$ the crack surface displacement $w(x,0)$ for the nonhomogeneous medium is greater than that for the homogeneous medium having the modulus $\mu(0) = \mu_0$. Since the stress intensity factor k_3 is related to the magnitude of the crack surface displacement derivative (see (41), (42) and (50)), it would, therefore, be expected that (for $\beta < 0$) at $x=0$ k_3 for the nonhomogeneous medium would be greater than $p_0 \sqrt{c}$, the value for the corresponding homogeneous medium. Even though near $x=b$ $w(x,0)$ is considerably greater than that near $x=0$, it is still smaller than the displacement for the homogeneous medium having $\mu = \mu(b)$ which also has $k_3(b) = p_0 \sqrt{c}$. With (41), this would then explain the trend for the stress intensity factor at $x=b$ shown in Fig. 2, namely that $k_3(b) < p_0 \sqrt{c}$.

Some sample results for the crack surface displacement in bonded nonhomogeneous half planes with a crack along $0 < x < b$ are shown in Fig. 4.

For uniform crack surface traction $\sigma_{1yz}(x,0) = -p_0$ Tables 1 and 2 show the calculated stress intensity factors normalized as

$$\frac{k_3(a)}{p_0 \sqrt{c}} = k(a) \quad , \quad \frac{k_3(b)}{p_0 \sqrt{c}} = k(b) \quad . \quad (60)$$

Aside from the validity of the general trends given in Fig. 2 for the infinite medium, these results also conform to the broad principle that in bonded nonhomogeneous solids as the crack tip approaches the interface the corresponding stress intensity factor tends to decrease if the crack lies in the medium with the smaller shear modulus and increase if the crack lies in the stiffer medium.

It should perhaps be pointed out that even though the main result of this study namely, that the square-root nature of the stress singularity is unaffected by the "kink" in $\mu(x)$, is based on a specific choice of the shear modulus ($\mu_0 e^{\beta x}$ for $x > 0$, $\mu_0 e^{\gamma x}$ for $x < 0$, $\beta \neq \gamma$), clearly the conclusion should be valid for any continuous function $\mu(x)$. One may, therefore, also conclude that the expression

$$k_3(0) = \lim_{x \rightarrow 0} \mu(x) \sqrt{2x} \frac{\partial}{\partial x} w(x, 0)$$

for the stress intensity factor at a crack tip $x=0$ is valid for any $\mu(x)$ which is continuous at $x=0$.

Acknowledgements. This study was performed at the Fraunhofer-Institut für Festkörpermechanik in Freiburg, Germany while the author was an Alexander von Humboldt Senior U.S. Scientist Awardee. The author would also like to thank Dr. A.C. Kaya for carrying out the numerical calculations.

References

1. T.S. Cook and F. Erdogan, "Stresses in bonded materials with a crack perpendicular to the interface", Int. J. Engng. Sci., Vol. 10, pp. 667-697, 1972.
2. F. Erdogan and T.S. Cook, "Antiplane shear cracks terminating at and going through a bimaterial interface", Int. J. of Fracture, Vol. 10, pp. 227-240, 1974.
3. R.S. Dhalival and B.M. Singh, "On the theory of elasticity of a nonhomogeneous medium", Journal of Elasticity, Vol. 8, pp. 211-219, 1978.
4. F. Delale and F. Erdogan, "The crack problem for a nonhomogeneous plane", ASME Journal of Applied Mechanics, Vol. 50, pp. 609-614, 1983.
5. N.I. Muskhelishvili, Singular Integral Equations, P. Noordhoff, Groningen, Holland, 1953.
6. F. Erdogan, "Mixed boundary value problems in mechanics", Mechanics Today, S. Nemat-Nasser, ed. Vol. 4, pp. 1-81, 1978.

Table 1. Stress intensity factor ratio $k_3/p_0\sqrt{c}$ in bonded nonhomogeneous half planes.

d/c	1.0		1.1		1.25		1.5		2.		5.	
	k(a)	k(b)	k(a)	k(b)	k(a)	k(b)	k(a)	k(b)	k(a)	k(b)	k(a)	k(b)
βc												
-2.0	2.197	0.576	1.813	0.571	1.576	0.566	1.401	0.561	1.284	0.558	1.238	0.556
-1.5	1.943	0.666	1.684	0.657	1.514	0.649	1.377	0.641	1.270	0.633	1.211	0.629
-1.0	1.635	0.783	1.494	0.772	1.395	0.762	1.309	0.750	1.231	0.738	1.165	0.727
-0.5	1.303	0.909	1.252	0.902	1.216	0.894	1.183	0.885	1.149	0.874	1.104	0.857
-0.25	1.143	0.961	1.122	0.958	1.108	0.954	1.096	0.949	1.082	0.943	1.062	0.932
-0.1	1.054	0.986	1.047	0.984	1.042	0.983	1.038	0.981	1.034	0.979	1.028	0.975
0.	1.	1.	1.	1.	1.	1.	1.	1.	1.	1.	1.	1.
0.1	0.952	1.015	0.958	1.016	0.962	1.018	0.965	1.019	0.968	1.020	0.971	1.023
0.25	0.889	1.038	0.901	1.041	0.909	1.043	0.915	1.046	0.921	1.049	0.927	1.054
0.5	0.799	1.074	0.820	1.078	0.831	1.083	0.841	1.087	0.848	1.092	0.854	1.098
1.0	0.664	1.136	0.693	1.142	0.707	1.149	0.717	1.155	0.723	1.160	0.726	1.163
1.5	0.570	1.185	0.601	1.192	0.615	1.199	0.623	1.204	0.627	1.208	0.629	1.210
2.0	0.503	1.218	0.535	1.224	0.546	1.230	0.553	1.234	0.556	1.237	0.556	1.238

Table 2. Stress intensity factor ratio $k_3/\rho_0\sqrt{c}$ in bonded nonhomogeneous half planes.

d/c	1.0		1.1		1.25		1.5		2		5	
	k(a)	k(b)	k(a)	k(b)	k(a)	k(b)	k(a)	k(b)	k(a)	k(b)	k(a)	k(b)
βc												
-0.1	1.034	0.977	1.032	0.976	1.030	0.976	1.029	0.975	1.027	0.974	1.025	0.973
-0.25	1.082	0.937	1.075	0.936	1.071	0.935	1.066	0.933	1.062	0.932	1.056	0.929
-0.5	1.155	0.867	1.139	0.865	1.128	0.863	1.118	0.861	1.109	0.858	1.099	0.855
-1.0	1.273	0.737	1.237	0.735	1.213	0.733	1.192	0.730	1.175	0.728	1.163	0.726
-1.5	1.363	0.635	1.305	0.633	1.268	0.632	1.240	0.631	1.220	0.629	1.210	0.629
-2.0	1.423	0.559	1.345	0.558	1.298	0.558	1.265	0.557	1.245	0.556	1.238	0.556
-0.25	0.975	0.906	0.999	0.909	1.015	0.912	1.028	0.916	1.040	0.920	1.053	0.927
-1.0	0.950	0.713	1.036	0.716	1.087	0.719	1.124	0.722	1.150	0.724	1.163	0.726
-2.0	0.947	0.553	1.094	0.554	1.167	0.555	1.211	0.556	1.233	0.556	1.238	0.556
-0.25	1.093	0.941	1.084	0.940	1.077	0.938	1.072	0.936	1.066	0.934	1.057	0.929
-1.0	1.329	0.743	1.276	0.740	1.241	0.737	1.210	0.733	1.184	0.730	1.164	0.726
-2.0	1.530	0.561	1.411	0.560	1.338	0.559	1.284	0.557	1.250	0.557	1.238	0.556
-0.25	1.261	0.999	1.207	0.990	1.171	0.981	1.140	0.971	1.109	0.958	1.067	0.535
-1.0	2.317	0.848	1.881	0.820	1.630	0.794	1.437	0.770	1.283	0.747	1.166	0.727
-2.0	3.665	0.600	2.440	0.584	1.879	0.573	1.527	0.565	1.316	0.559	1.238	0.556
1	1.106	1.038	1.072	1.033	1.052	1.027	1.035	1.021	1.020	1.014	1.004	1.003
-1	0.907	0.966	0.935	0.970	0.952	0.975	0.967	0.980	0.980	0.987	0.996	0.997
5	1.383	1.097	1.213	1.076	1.132	1.057	1.077	1.040	1.038	1.023	1.005	1.004
-5	0.737	0.929	0.834	0.940	0.888	0.952	0.931	0.964	0.965	0.978	0.995	0.996
0.25	0.913	1.049	0.918	1.050	0.921	1.051	0.923	1.052	0.925	1.053	0.927	1.055
1.0	0.704	1.154	0.715	1.157	0.720	1.159	0.723	1.161	0.725	1.162	0.726	1.163
2.0	0.537	1.232	0.549	1.234	0.553	1.236	0.555	1.237	0.556	1.238	0.556	1.238
0.25	0.839	1.019	0.868	1.024	0.886	1.030	0.901	1.036	0.913	1.044	0.926	1.053
1.0	0.595	1.111	0.657	1.123	0.687	1.135	0.707	1.147	0.720	1.157	0.726	1.163
2.0	0.446	1.201	0.513	1.213	0.537	1.223	0.550	1.231	0.555	1.237	0.556	1.238
0.25	0.981	1.074	0.961	1.070	0.950	1.067	0.941	1.063	0.934	1.059	0.928	1.055
1.0	0.802	1.184	0.758	1.177	0.742	1.172	0.733	1.168	0.728	1.165	0.726	1.163
2.0	0.618	1.250	0.573	1.245	0.562	1.241	0.558	1.239	0.556	1.238	0.556	1.238
0.25	0.908	1.047	0.915	1.048	0.919	1.049	0.922	1.051	0.925	1.052	0.927	1.054
1.0	0.696	1.151	0.710	1.154	0.717	1.157	0.722	1.159	0.725	1.162	0.726	1.163
2.0	0.530	1.229	0.546	1.232	0.552	1.235	0.555	1.237	0.556	1.238	0.556	1.238

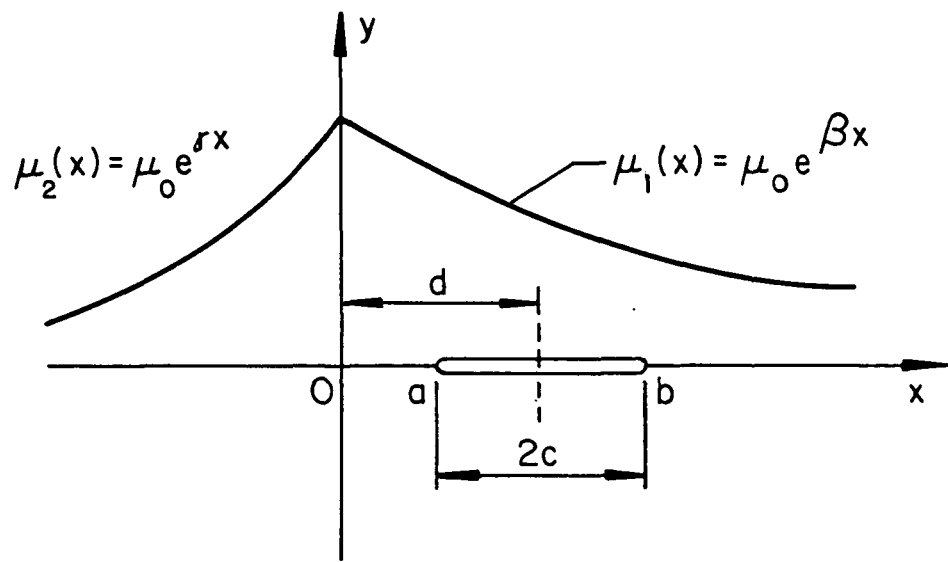


Fig. 1 Geometry for bonded nonhomogeneous half planes.

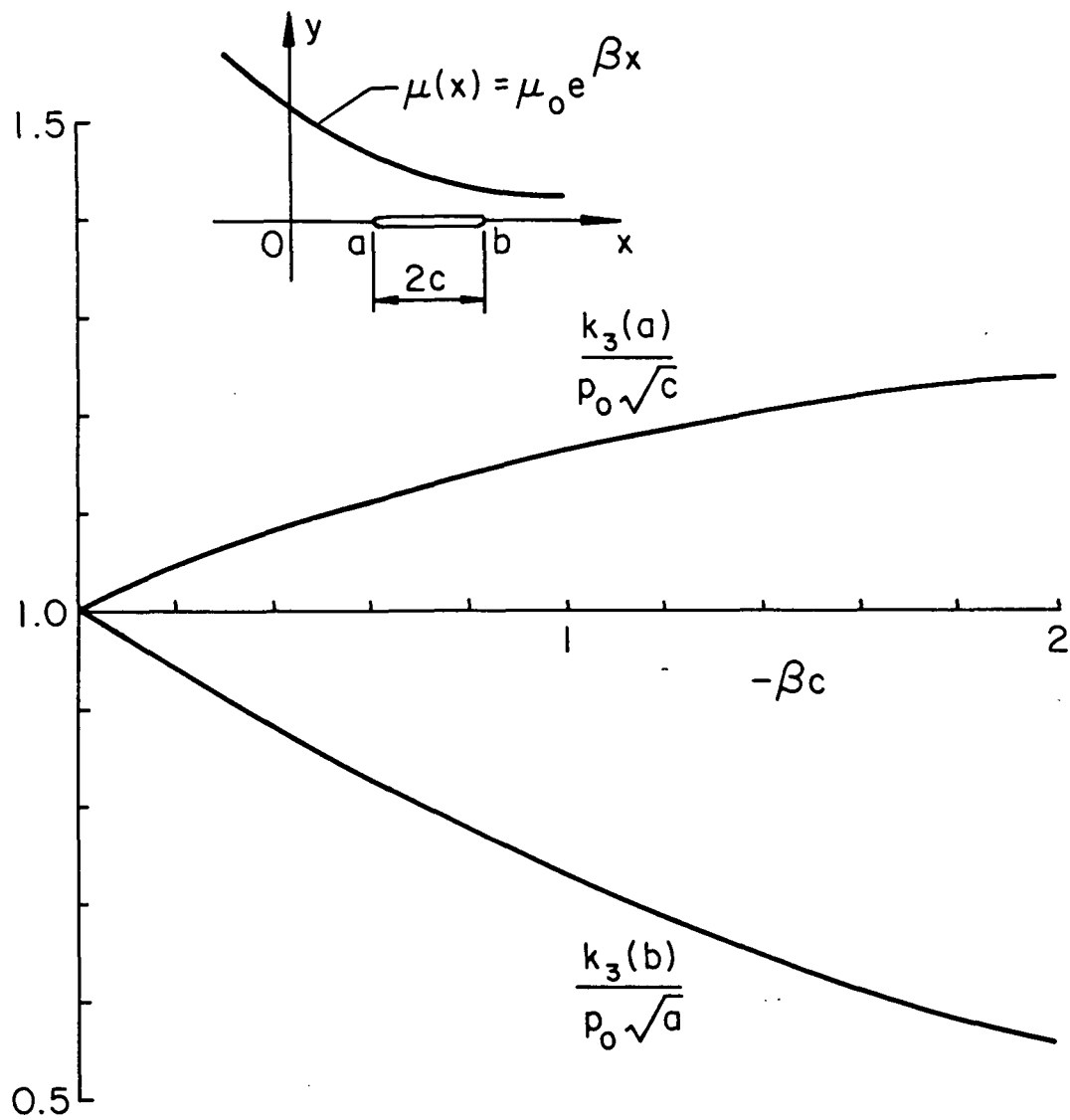


Fig. 2 Stress intensity factors for an infinite nonhomogeneous plane subjected to uniform crack surface traction $\sigma_{yz}(x,0) = -p_0$.

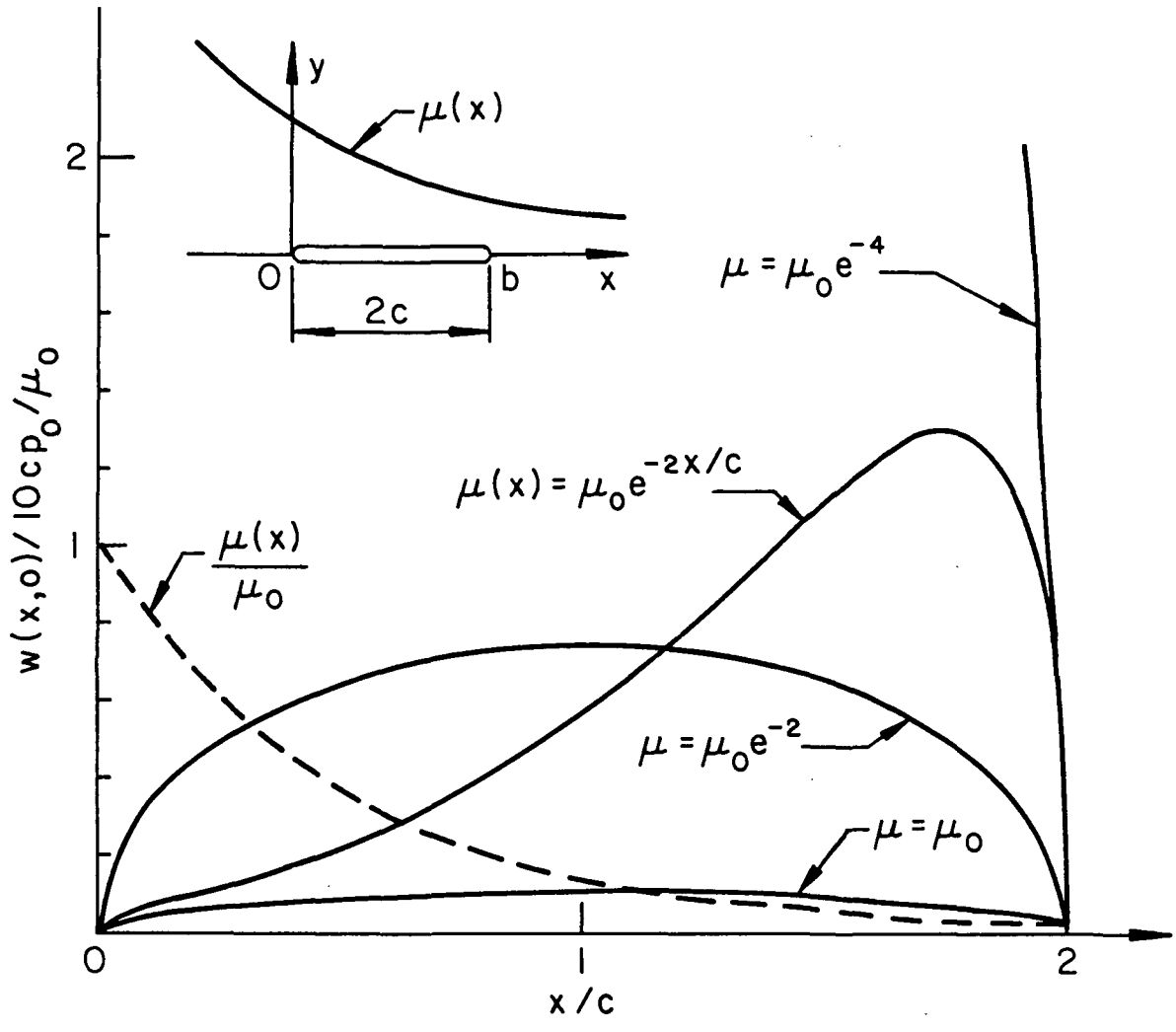


Fig. 3 Crack surface displacement in an infinite nonhomogeneous plane under uniform crack surface shear loading $\sigma_{yz}(x,0) = -p_0$; shear modulus $\mu(x) = \mu_0 e^{\beta x}$, $\beta c = -2$.

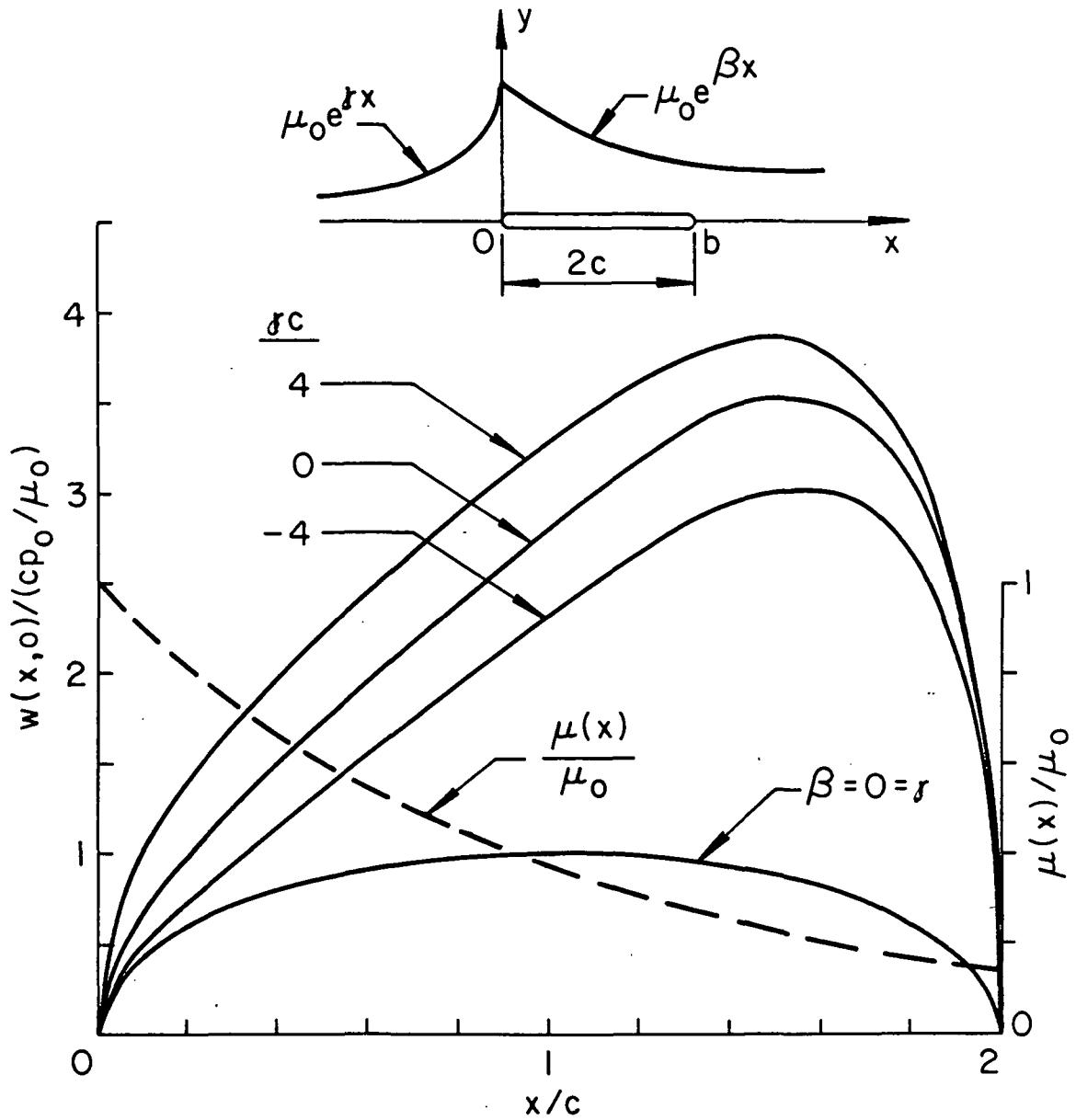


Fig. 4 Crack surface displacement in bonded nonhomogeneous half planes under uniform antiplane shear loading $\sigma_{1yz}(x, 0) = -p_0$; $\mu(x) = \mu_0 \exp(\beta x)$, $x > 0$; $\mu(x) = \mu_0 \exp(\gamma x)$, $x < 0$, $\beta = -1$.